The value of [18F]FDG-PET in the diagnosis of large-vessel vasculitis and the assessment of activity and extent of disease

Martin A. Walter[1], Ralph A. Melzer[2], Christian Schindler[3], Jan Müller-Brand[1], Alan Tyndall[2], Egbert U. Nitzsche[1]

[1] Institute of Nuclear Medicine, University Hospital Basel, Petersgraben 4, 4031 Basel, Switzerland
[2] Division of Rheumatology, University Hospital Basel, Switzerland
[3] Institute of Social and Preventive Medicine, University Hospital Basel, Switzerland

Abstract. *Purpose:* This study was performed to investigate the value of [18F]-fluorodeoxyglucose positron emission tomography ([18F]FDG-PET) in the diagnosis of large-vessel vasculitis and the assessment of activity and extent of disease.
Methods: Twenty-six consecutive patients (21 females, 5 males; median age – years, range 17–86 years) with giant cell arteritis or Takayasu's arteritis were examined with [18F]FDG-PET. Follow-up scans were performed in four patients. Twenty-six age- and gender-matched controls (21 females, 5 males; median age 71 years, range 17–86 years) were included. The severity of large-vessel [18F]FDG uptake was visually graded using a four-point scale. C-reactive protein (CRP) and the erythrocyte sedimentation rate (ESR) were measured and correlated with [18F]FDG-PET results by logistic regression.
Results: [18F]FDG-PET revealed pathological findings in 18 of 26 patients. Three scans were categorised as grade I, 12 as grade II and 3 as grade III arteritis. Visual grade was significantly correlated with both CRP and ESR levels (p=0.002 and 0.007 respectively; grade I: CRP 4.0 mg/l, ESR 6 mm/h; grade II: CRP 37 mg/l, ESR 46 mm/h; grade III: CRP 172 mg/l, ESR 90 mm/h). Overall sensitivity was 60% (95% CI 40.6–77.3%), specificity 99.8% (95% CI 89.1–100%), positive predictive value 99.7% (95% CI 77–100%), negative predictive value 67.9% (95% CI 49.8–80.9%) and accuracy 78.6% (95% CI 65.6–88.4%). In patients presenting with a CRP <12 mg/l or an ESR <12 mm/h, logistic regression revealed a sensitivity of less than 50%. In patients with high CRP/ESR levels, sensitivity was 95.5%/80.7%.
Conclusion: [18F]FDG-PET is highly effective in assessing the activity and the extent of large-vessel vasculitis. Visual grading was validated as representing the severity of inflammation. Its use is simple and provides high specificity, while high sensitivity is achieved by scanning in the state of active inflammation.

Keywords: Large-vessel vasculitis – Giant cell arteritis – Takayasu's arteritis – FDG – PET

Introduction

The diagnosis of large-vessel vasculitis and the assessment of its activity and extent remain challenging, especially in patients presenting with a constellation of non-specific symptoms and laboratory tests. The standard diagnostic procedures include biopsy, angiography, ultrasound and magnetic resonance angiography (MRA); nevertheless, these procedures are invasive, are largely operator-dependent or document only morphological changes, such as stenosis, occlusion and aneurysmal transformation, which mainly occur in late stages of the disease [1–5].

Positron emission tomography (PET) is an operator-independent, non-invasive metabolic imaging modality based on the regional distribution of [18F]-fluorodeoxyglucose ([18F]FDG) which plays a major role in the management of oncology patients. However, activated inflammatory cells have also been shown to overexpress glucose transporters and to accumulate increased amounts of glucose and structurally related substances such as [18F]FDG [6, 7]; therefore, [18F]FDG-PET may become a useful tool in the evaluation of Takayasu's arteritis (TA) and giant cell arteritis (GCA). Nevertheless, the lack of accurate criteria for vasculitis imaging based on [18F]FDG-PET has restricted its use so far. This study therefore aimed to explore the properties of [18F]FDG-PET in the detection of large-vessel vasculitis and in the assessment of the activity and extent of disease.

Martin A. Walter (✉)
Institute of Nuclear Medicine, University Hospital Basel,
Petersgraben 4, 4031 Basel, Switzerland
e-mail: m.a.walter@gmx.net
Tel.: +41-61-2655684, Fax: +41-61-2654897

Materials and methods

Patients

Throughout a period of 24 months (from April 2002 to April 2004), 26 consecutive patients (21 females, 5 males; median age 71 years, range 17–86 years) with a clinical diagnosis of GCA (20 patients) or TA (six patients) were examined with [18F]FDG-PET. Follow-up scans were performed in four patients. Twenty-one of the 30 scans (70%) were performed under simultaneous glucocorticosteroid treatment. The classification as GCA or TA was made according to the ACR classification criteria [8, 9] and verified when at least three of the criteria were present. Patients were referred by the Department of Rheumatology of the University Medical Centre. Patient characteristics and baseline investigation results are shown in Table 1.

Additionally, in order to determine normal values for vascular uptake on [18F]FDG-PET, an age- and gender-matched reference group of 26 patients (21 females, 5 males; median age 71 years, range 17–86 years) who underwent [18F]FDG-PET for malignancy were visually scored.

Biochemical investigations

The serum levels of CRP (Tina-Quant, Roche, Switzerland; reference range <10 mg/l), haemoglobin (ADVIA 120, Bayer, Switzerland; reference range 120–160 g/l), leucocytes (ADVIA 120; reference range $3.5–10 \times 10^9 \ l^{-1}$) and thrombocytes (ADVIA 120; reference range 150–$450 \times 10^9 \ l^{-1}$) and the erythrocyte sedimentation rate (Westergren method) were measured in the week of the [18F]FDG-PET scan to assess the severity of systemic inflammation.

Table 1. Patient characteristics and baseline investigation results

	All patients (n=26)	Giant cell arteritis (n=20)	Takayasu's arteritis (n=6)
Females/males	21/5	15/5	6/0
Age (years)	71 (17–86)	72 (53–86)	40 (17–74)
Duration of disease (year)	1.0 (0.1–24.4)	1.0 (0.1–3.8)	2.9 (0.4–24.4)
Pre-PET lab results			
ESR (mm/h)	35 (4–130)	43 (4–130)	18 (5–75)
CRP (mg/l)	27.4 (0.3–220)	32.5 (1.8–220)	3 (0.3–29)
Haemoglobin (mg/dl)	13.1 (8.1–14.8)	11.8 (8.1–14.8)	13.1 (8.6–13.6)
Leucocytes ($\times 10^9 \ l^{-1}$)	7.8 (5.1–17.4)	9.6 (6.3–17.4)	7.1 (5.1–7.5)
Thrombocytes ($\times 10^9 \ l^{-1}$)	369 (142–686)	409 (142–686)	279 (235–415)

Values are expressed as median (range). The reference ranges for the laboratory values are: CRP <10 mg/l, haemoglobin 120–160 g/l, leucocytes 3.5–$10.00 \times 10^9 \ l^{-1}$, thrombocytes 150–$450 \times 10^9 \ l^{-1}$
ESR erythrocyte sedimentation rate, *CRP* C-reactive protein

PET acquisition

[18F]FDG-PET was performed after patients had fasted for 12 h using a dedicated full-ring PET camera system (ECAT EXACT-922/47, Siemens, Germany) with 32 rings and an axial field of view of 16 cm. The serum glucose level was measured before [18F]FDG administration in all patients and was below 180 mg/dl (Glucometer Elite, Bayer Diagnostics, UK). Acquisition was started 45 min after intravenous injection of 5 MBq/kg body weight of [18F]FDG with the patient in the supine position. We performed whole-body scans using 2D acquisition with 12–14 contiguous bed positions (8 min/bed position: 6-min emission scan and 2-min attenuation correction with a rotating 68Ge line sources). Iterative reconstruction of the transaxial slices was performed using the ordered subset–expectation maximisation (OS-EM) algorithm (two iterations, eight subsets).

Evaluation and scoring of data

Images were judged by two experienced nuclear medicine physicians blinded to the clinical and laboratory data. At a time interval of 1 month, the same two observers evaluated the same images blinded to the previous judgment. The severity of large-vessel [18F]FDG uptake was visually graded using a four-point scale (Fig. 1a): 0, no uptake present; I, low-grade uptake (uptake present but lower than liver uptake); II, intermediate-grade uptake (similar to liver uptake); III, high-grade uptake (uptake higher than liver uptake).

Statistical evaluation

All data are expressed as median (range) in text and tables. To ascertain whether CRP and ESR levels were positively associated with the grade of [18F]FDG uptake, the Jonckheere-Terpstra test was used. Logistic regression was used to assess the effects of CRP and ESR on the sensitivity of [18F]FDG-PET. Statistical significance was defined as $p < 0.05$. Data were analysed using Statistica Version 6.0 for Windows (StatSoft Inc., Tulsa, USA).

Results

Reference group

Grade I [18F]FDG uptake was present in the ascending aorta in 20/26 (77%) patients, in the aortic arch in 17/26 (65%) and in the thoracic part of the descending aorta in 4/26 (15%). Visible [18F]FDG uptake in the abdominal part of the descending aorta or in one of the large aortic branches was not found in any of the control group, nor were there any instances of grade II or III uptake in controls. Therefore, in the present study, grade II or III uptake in the thoracic aorta and any visible uptake in other segments was considered as pathological and due to active arterial inflammation.

Assessment of activity

Thirty PET scans were performed (26 baseline and 4 follow-up studies) in the patients. Three scans were judged as grade I, 12 as grade II and 3 as grade III arteritis. Inter-

Fig. 1. a Examples of visual grading of
[^{18}F]FDG uptake. **b** Non-pathological
whole-body [^{18}F]FDG-PET scan. **c** Whole-
body [^{18}F]FDG-PET scan showing extensive
large-vessel arteritis
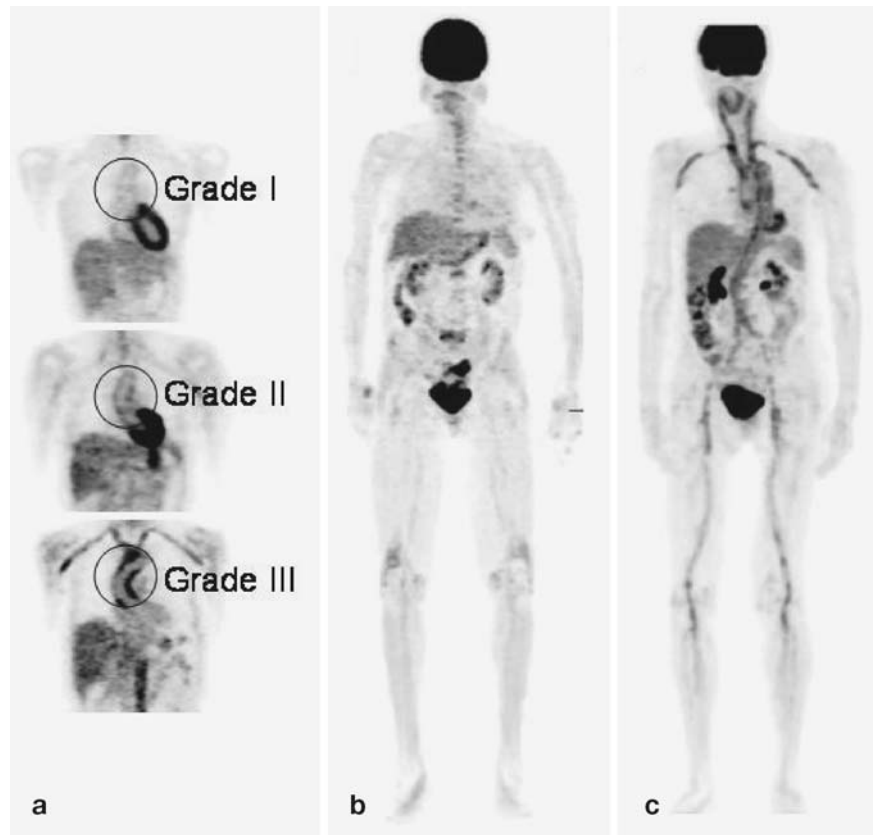
observer agreement regarding the severity score was obtained in 93.3% (28/30) of the scans, and the intra-observer reproducibility was 90% (27/30). The visual grade and the patient's ESR were significantly correlated: patients with grade I arteritis had an ESR of 6 mm/h (4–9 mm/h), patients with grade II arteritis had an ESR of 46 mm/h (6–130 mm/h) and patients with grade III arteritis showed an ESR of 90 mm/h (72–100 mm/h) (p=0.007; Fig. 2a). We also found a significant correlation between the visual grade and the patient's CRP: patients with grade I arteritis had a mean CRP of 4.0 mg/l (2–10 mg/l), grade II patients had a CRP of 37 mg/l (2–158 mg/l) and patients with grade III arteritis showed a CRP of 172 mg/l (95–220 mg/l) (p=0.002; Fig. 2b).

Follow-up PET studies were performed in four patients. All of them had received glucocorticosteroid drug treat-
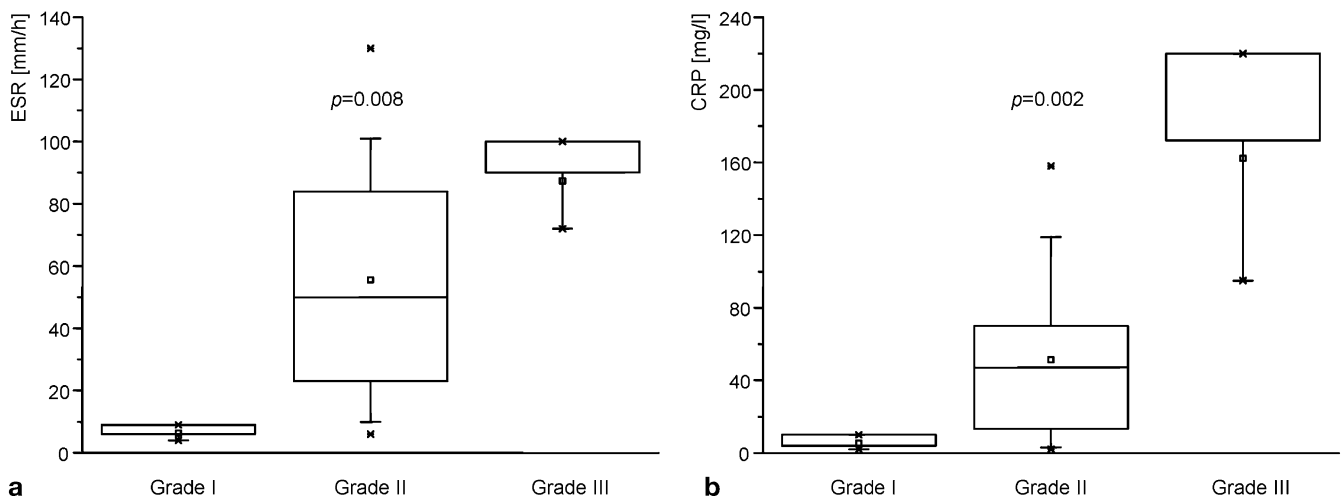
Fig. 2. Correlation of large-vessel [^{18}F]FDG uptake with ESR and CRP level. Based on the Jonckheere-Terpstra test, the grade of large-vessel [^{18}F]FDG uptake (grade I–III) was positively correlated with both ESR (**a**, p=0.007) and CRP level (**b**, p=0.002)

ment after the baseline study, resulting in clinical improvement and mean decreases of 31 mm/h in the ESR and 38 mg/l in CRP. Follow-up [18F]FDG-PET confirmed a marked reduction in disease activity (from grade II to I in three patients and from grade II to 0 in one patient) and extension (the number of affected segments in the four patients decreased from 28 in the baseline study to 15 in the follow-up study).

Assessment of diagnosis

In the study group, 18/30 scans showed pathological large-vessel [18F]FDG uptake, while in the control group 0/26 scans were found to be pathological due to active arterial inflammation. Statistical analysis revealed an overall sensitivity of 60% (95% CI 40.6–77.3%), a specificity of 99.8% (95% CI 89.1–100%), a positive predictive value of 99.7% (95% CI 77–100%), a negative predictive value of 67.9% (95% CI 49.8–80.9%) and an accuracy of 78.6% (95% CI 65.6–88.4%). Non-pathological [18F]FDG uptake (grade I uptake in the thoracic part of the aorta) was found in 2/30 studies, and 10/30 studies showed no visible [18F]FDG uptake. Overall, abnormal [18F]FDG uptake was present in 129/360 (35.8%) vascular regions studied (Table 2). For

Table 2. Results of [18F]FDG-PET scans (*n*=30)

	Baseline scan (*n*=26)	Follow-up scan (*n*=4)
PET scan under glucocorticosteroids	17	4
Diagnosis		
Inflammatory large-vessel [18F]FDG uptake	16	2
Activity		
[18F]FDG uptake		
Grade 0	10	2
Grade I	1	2
Grade II	12	0
Grade III	3	0
Extend of inflammatory [18F]FDG uptake		
Ascending aorta	15	2
Aortic arch	15	2
Brachiocephalic trunk	13	1
Common carotid arteries	12	0
Subclavian arteries	13	2
Axillary arteries	11	1
Descending aorta (thoracic part)	15	2
Descending aorta (abdominal part)	9	1
Iliac arteries	7	1
Femoral arteries	3	0
Popliteal arteries	2	0
Tibial/fibular arteries	2	0

Inflammatory large-vessel [18F]FDG uptake was defined as grade II or III uptake of the thoracic aorta or any visible uptake in the abdominal aorta or in one of the large aortic branches

patients presenting with an ESR <12 mm/h, logistic regression revealed a sensitivity of less than 50%. In patients with a high ESR, sensitivity increased to 80.7% (Fig. 3). Separate analysis in those with a high ESR revealed a sensitivity of 78.6% for patients suffering from GCA (22 scans) and 40.3% for patients suffering from TA (eight scans).

Compared with ESR, CRP showed a superior correlation with the sensitivity of [18F]FDG-PET. For patients presenting with a CRP <12 mg/l, logistic regression revealed [18F]FDG-PET to have a sensitivity of less than 50%. With high CRP levels, sensitivity increased to 95.5% (Fig. 3). Separate analysis revealed a sensitivity of 93.7% for patients suffering from GCA (22 scans) and 46.6% for patients suffering from TA (eight scans), at high CRP levels.

Ten of 21 PET scans (47.6%) with and eight of nine scans (88.9%) without simultaneous glucocorticosteroid treatment showed pathological large-vessel [18F]FDG uptake (*p*=0.034).

Assessment of disease extent

The extent of large-vessel vasculitis was assessed using MRA, ultrasound, temporal artery biopsy or aortic biopsy prior to [18F]FDG-PET. Thereby, 6/26 patients (23.1%) were diagnosed as having extensive inflammation (with involvement of the aorta and major aortic branches) while 20/26 (76.9%) were considered to have limited inflammation (involvement of the aorta without involvement of major aortic branches). [18F]FDG-PET confirmed the diagnosis of extensive disease in all six of the aforementioned patients (100%), revealing a median of 10 (5–13) affected vascular segments in this group. PET also confirmed the diagnosis of limited disease in 12/20 patients (60%), showing pathological [18F]FDG uptake in a median of 3 (0–19) vascular segments. Additionally, in 8 of 20 cases (40%), the diag-
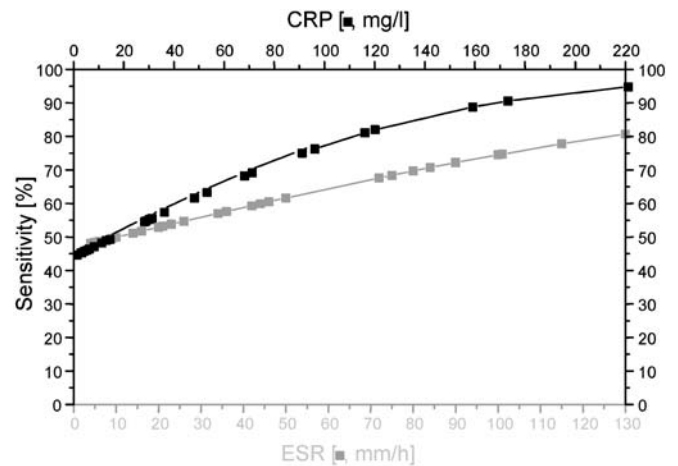
**Fig. 3.** Sensitivity of [18F]FDG-PET in detecting large-vessel vasculitis as a function of CRP and ESR levels (*black squares*, CRP; *grey squares*, ESR). Curve estimates were obtained from logistic regression models. High sensitivity for detection of large-vessel vasculitis is achieved at high CRP and ESR levels
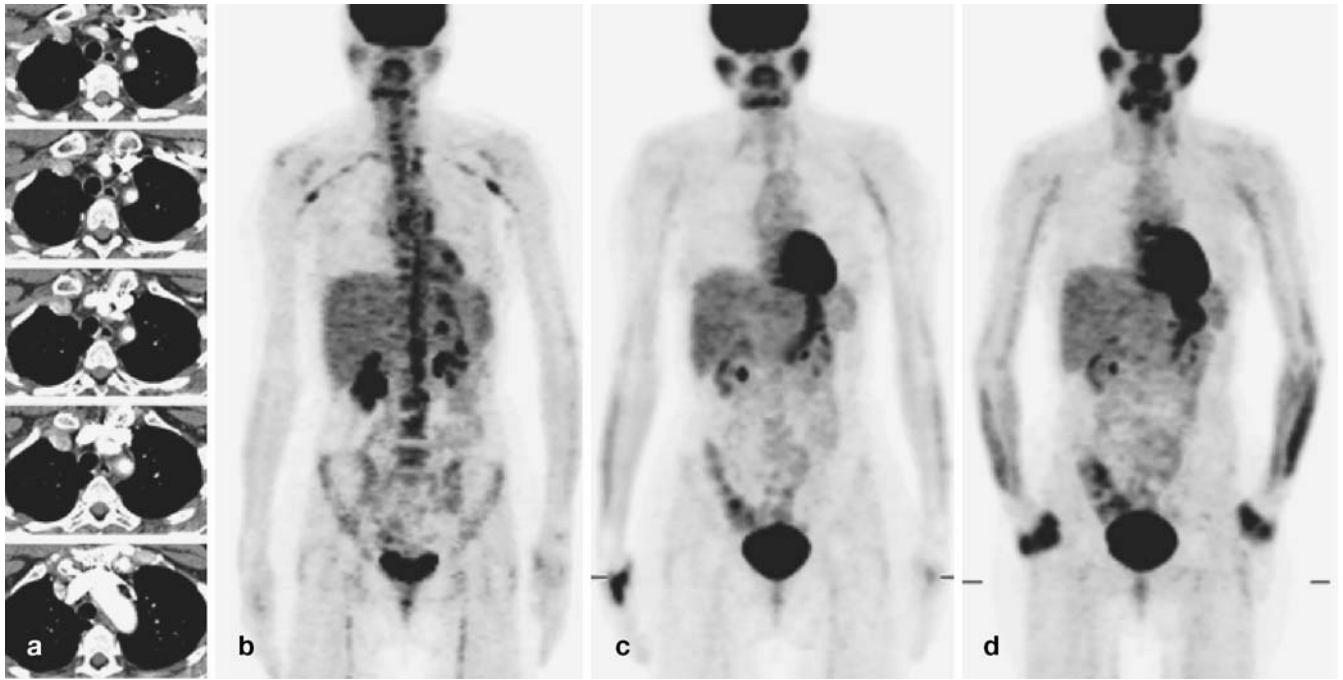
Fig. 4. a The abdominal and thoracic CT scan of a 52-year-old woman with rheumatoid arthritis, fever, night sweating and loss of weight showed no abnormalities. **b** In contrast, the PET scan revealed generalised bone marrow activation as a consequence of chronic inflammation and demonstrated pathological [^{18}F]FDG uptake in the vessel wall of the aorta and its main thoracic and abdominal branches. **c, d** In parallel with the distinct clinical improvement, this uptake decreased significantly after 9 (**c**) and 18 months (**d**) of glucocorticosteroid treatment
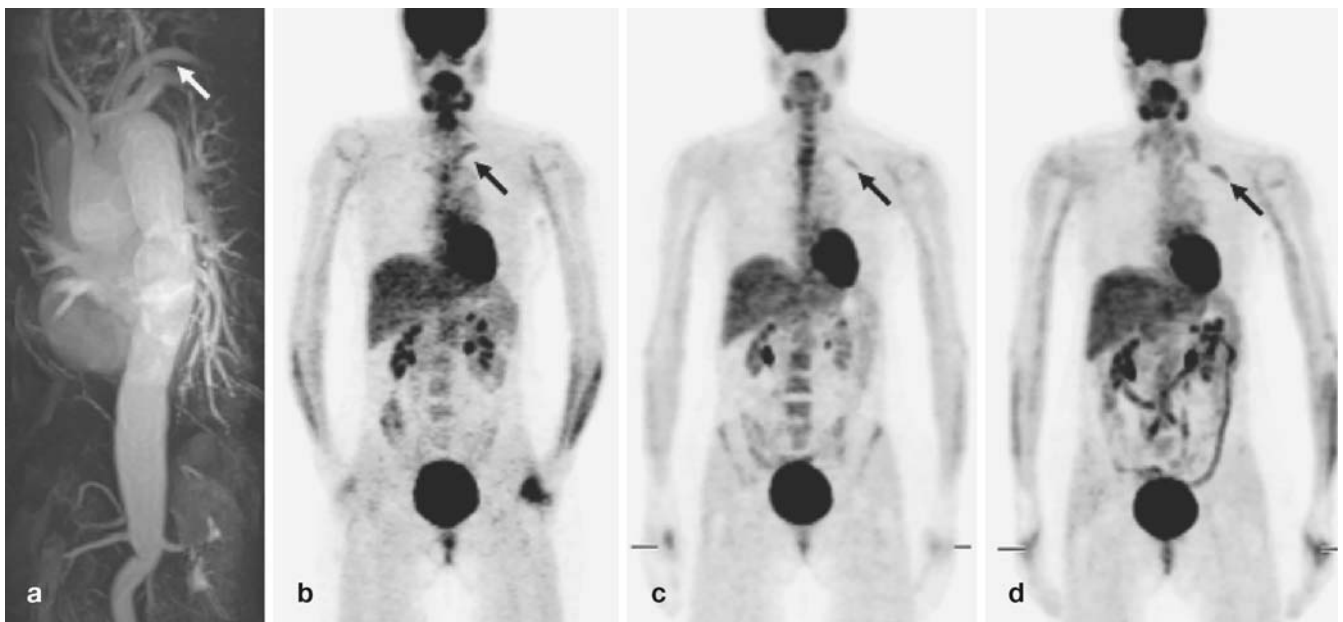
Fig. 5. a MRI of a 45-year-old female with known Takayasu's arteritis revealed no vascular wall thickening in any segment, while MRA demonstrated an aneurysmal aorta and a regular lumen of the left subclavian artery (*arrow*), indicating inactive disease. **b** In contrast, the PET scan showed generalised bone marrow activation as a consequence of chronic inflammation and demonstrated patholog- ical [^{18}F]FDG uptake in the wall of the left subclavian artery (*arrow*). **c, d** This uptake decreased significantly after 9 months of gluco- corticosteroid treatment (**c**). However, inflammation of the distal subclavian artery segment was found (**c**, *arrow*), which increased significantly after reduction of glucocorticosteroids (**d**, *arrow*)

nosis of limited disease was upgraded to extensive disease based on findings in respect of the aortic branches identified as involved on [^{18}F]FDG-PET.

Discussion

Large-vessel [^{18}F]FDG uptake is positively correlated with the level of acute phase reactant markers in patients with large-vessel vasculitis. Consequently, high sensitivities are achieved in the state of active inflammation. Additionally, the possibility of scanning the whole body improves the determination of the disease extent.

The ability to visualise [^{18}F]FDG accumulation by activated inflammatory cells makes PET a promising modality for the management of primary inflammatory diseases. The correlation of [^{18}F]FDG uptake with the level of biochemical inflammatory markers has led to the validation of [^{18}F]FDG-PET for the assessment of severity of polymyalgia rheumatica [10]. In addition, the use of [^{18}F]FDG-PET in GCA or TA has recently been suggested by numerous case reports [11–18] and observations in a limited number of patients [19, 20]. Larger studies, however, are few in number and have not yet conclusively verified the relation between [^{18}F]FDG uptake and severity of GCA and TA. In 25 patients with either GCA or polymyalgia rheumatica, no significant correlation was found between [^{18}F]FDG-PET results and inflammatory markers [21]. In a further study, 18 patients with TA were classified into [^{18}F]FDG-PET-positive and -negative groups; the [^{18}F]FDG-PET-positive patients showed significantly higher CRP and ESR levels than those with a negative scan [22].

In the present study we used a four-point scale (Fig. 1a) to grade the large-vessel [^{18}F]FDG uptake into none (grade 0), lower than liver uptake (grade I), similar to liver uptake (grade II) and higher than liver uptake (grade III). This scale was proposed by Meller et al. [23], who reported no association with their patients' clinical or biochemical data. In contrast, we found a highly significant correlation between visual score and both CRP and ESR (Fig. 2); hence, this study is the first report to validate the visual arteritis score. With the use of this score, high inter-observer agreement and very good intra-observer reproducibility were achieved.

Nevertheless, the major advantage of the visual arteritis score is the achievement of high specificity for active large-vessel inflammation by excluding [^{18}F]FDG accumulation due to active atherosclerosis. Atherosclerotic plaques also accumulate glucose analogues [24] and modest large-vessel [^{18}F]FDG accumulation consequently occurs at the level of the major vessels in about 50% of all PET scans [25, 26]. Accordingly, in our control group grade I vessel uptake was frequently found in the thoracic part of the aorta. Thus, only grade II or III uptake in the thoracic aorta and any visible uptake in other segments should be judged to represent active large-vessel inflammation. It is of note that grade II or III [^{18}F]FDG uptake regularly normalised in the follow-up scans, which strongly argues against other than primary inflammatory causes.

In order to draw appropriate conclusions from the [^{18}F]FDG-PET result, consensual data on specificity and sensitivity are required; however, the currently available data are limited and controversial. A study in 15 patients with early untreated TA or GCA concluded that [^{18}F]FDG-PET identified more vascular regions than did MRA, though sensitivity values were not provided as only PET-positive patients were included [23]. Sensitivities of 56% and 64%, respectively, were found for large-vessel [^{18}F]FDG uptake in the thorax and lower extremities in 25 patients with either polymyalgia rheumatica or GCA [21]; no significant correlation between [^{18}F]FDG-PET results and inflammatory markers was found. Nonetheless, in another study in 18 patients with TA, a sensitivity of 92% was reported [22]. Our results offer an explanation for these discrepant findings. With an overall sensitivity of 60%, we were able to show that the sensitivity strongly depends on the present severity of inflammation as assessed by the CRP or ESR levels (Fig. 3). Compared with ESR, CRP is a better predictor of the sensitivity of [^{18}F]FDG-PET, and a 95.5% sensitivity can be achieved at high CRP levels. However, several authors have previously reported that, unlike inflammatory markers of GCA, those of TA do not always reflect the inflammatory activity of the disease [27]. This is also reflected by our finding of a better correlation between biochemical inflammatory markers and the sensitivity of [^{18}F]FDG-PET in patients suffering from GCA. Nevertheless, this report is the first to illuminate the relation between severity of inflammation and sensitivity of [^{18}F]FDG-PET. Based on our findings we suggest that, in contrast to studies that have proposed the use of [^{18}F]FDG-PET for the diagnosis of large-vessel vasculitis even in the absence of elevated inflammatory markers [22], we recommend its use mainly in active inflammation and, if possible, after the withdrawal of glucocorticosteroid treatment.

Extracranial involvement is commonly asymptomatic and most often discovered only after serious complications such as strokes, myocardial infarction, ruptured aortic aneurysm or aortic dissection. [28–31]. However, the standard diagnostic modalities such as biopsy, angiography, ultrasound and MRA are commonly unable to demonstrate the full extent of vascular involvement in large-vessel arteritis [1–5]. In contrast, [^{18}F]FDG-PET offers the possibility of demonstrating the overall topography of large-vessel involvement as it can visually represent the whole body in a single image (Figs. 1b, c, 4, 5). In this study, [^{18}F]FDG-PET confirmed the previous diagnosis in 18 of 26 patients and found unexpected extensive involvement in eight patients. These results are comparable to prior findings and highlight the major advantage of [^{18}F]FDG-PET in the work-up of patients with large-vessel vasculitis [11, 22, 23, 32, 33]. The assessment of extent, however, is limited to extracranial vessels, as the elevated physiological glucose metabolism in the brain obscures [^{18}F]FDG uptake in adjacent structures [34].

Nevertheless, if our results can be confirmed by other investigators, [^{18}F]FDG-PET may have an important role in the non-invasive evaluation of large-vessel vasculitis and probably allows a better understanding of the disease

process and its distribution. The main application will be in the evaluation of atypical presentations of large-vessel vasculitis and in the monitoring of response to anti-inflammatory treatment and disease recurrence. [^{18}F]FDG-PET is of potential value in reducing the time to diagnosis (by guiding the selection of the site of choice for a diagnostic biopsy) and in limiting the number of angiograms performed on a patient once the diagnosis has been established. Prospective intervention studies, however, will be helpful in order to further clarify the role of [^{18}F]FDG-PET in large-vessel inflammation.

In conclusion, [^{18}F]FDG-PET is highly effective in assessing the activity and the extent of large-vessel vasculitis. A visual grading scale was validated as representing the severity of inflammation. Its use is simple and it provides high specificity, while high sensitivity is achieved by PET scanning during the active inflammatory phase.

References

1. Salvarani C, Silingardi M, Ghirarduzzi A, Lo Scocco G, Macchioni P, Bajocchi G, et al. Is duplex ultrasonography useful for the diagnosis of giant-cell arteritis? Ann Intern Med 2002; 137:232–8.
2. Blockmans D. Utility of imaging studies in assessment of vascular inflammation. Cleve Clin J Med 2002;69 Suppl 2:SII95–9.
3. Tso E, Flamm SD, White RD, Schvartzman PR, Mascha E, Hoffman GS. Takayasu arteritis: utility and limitations of magnetic resonance imaging in diagnosis and treatment. Arthritis Rheum 2002;46:1634–42.
4. Kissin EY, Merkel PA. Diagnostic imaging in Takayasu arteritis. Curr Opin Rheumatol 2004;16:31–7.
5. Seo P, Stone JH. Large-vessel vasculitis. Arthritis Rheum 2004; 51:128–39.
6. Ishimori T, Saga T, Mamede M, Kobayashi H, Higashi T, Nakamoto Y, et al. Increased ^{18}F-FDG uptake in a model of inflammation: concanavalin A-mediated lymphocyte activation. J Nucl Med 2002;43:658–63.
7. Jones HA, Cadwallader KA, White JF, Uddin M, Peters AM, Chilvers ER. Dissociation between respiratory burst activity and deoxyglucose uptake in human neutrophil granulocytes: implications for interpretation of ^{18}F-FDG PET images. J Nucl Med 2002;43:652–7.
8. Hunder GG, Bloch DA, Michel BA, Stevens MB, Arend WP, Calabrese LH, et al. The American College of Rheumatology 1990 criteria for the classification of giant cell arteritis. Arthritis Rheum 1990;33:1122–8.
9. Arend WP, Michel BA, Bloch DA, Hunder GG, Calabrese LH, Edworthy SM, et al. The American College of Rheumatology 1990 criteria for the classification of Takayasu arteritis. Arthritis Rheum 1990;33:1129–34.
10. Moosig F, Czech N, Mehl C, Henze E, Zeuner RA, Kneba M, et al. Correlation between 18-fluorodeoxyglucose accumulation in large vessels and serological markers of inflammation in polymyalgia rheumatica: a quantitative PET study. Ann Rheum Dis 2004;63:870–3.
11. Turlakow A, Yeung HW, Pui J, Macapinlac H, Liebovitz E, Rusch V, et al. Fludeoxyglucose positron emission tomography in the diagnosis of giant cell arteritis. Arch Intern Med 2001; 161:1003–7.
12. Blockmans D, Van Moer E, Dehem J, Feys C, Mortelmans L. Positron emission tomography can reveal abdominal periaortitis. Clin Nucl Med 2002;27:211–2.
13. Wenger M, Gasser R, Donnemiller E, Erler H, Glossmann H, Patsch JR, et al. Images in cardiovascular medicine. Generalized large vessel arteritis visualized by 18fluorodeoxyglucose-positron emission tomography. Circulation 2003;107:923.
14. Brodmann M, Lipp RW, Aigner R, Pilger E. Positron emission tomography reveals extended thoracic and abdominal periaortitis. Vasc Med 2003;8:127–8.
15. Wiest R, Gluck T, Schonberger J, Scholmerich J, Eilles C, Muller-Ladner U. Clinical image: occult large vessel vasculitis diagnosed by PET imaging. Rheumatol Int 2001;20:250.
16. De Winter F, Petrovic M, Van de Wiele C, Vogelaers D, Afschrift M, Dierckx RA. Imaging of giant cell arteritis: evidence of splenic involvement using FDG positron emission tomography. Clin Nucl Med 2000;25:633–4.
17. Hara M, Goodman PC, Leder RA. FDG-PET finding in early-phase Takayasu arteritis. J Comput Assist Tomogr 1999;23:16–8.
18. Malik IS, Harare O, AL-Nahhas, Beatt K, Mason J. Takayasu's arteritis: management of left main stem stenosis. Heart 2003; 89:e9.
19. Bleeker-Rovers CP, Bredie SJ, van der Meer JW, Corstens FH, Oyen WJ. Fluorine 18 fluorodeoxyglucose positron emission tomography in the diagnosis and follow-up of three patients with vasculitis. Am J Med 2004;116:50–3.
20. Blockmans D, Maes A, Stroobants S, Nuyts J, Bormans G, Knockaert D, et al. New arguments for a vasculitic nature of polymyalgia rheumatica using positron emission tomography. Rheumatology (Oxford) 1999;38:444–7.
21. Blockmans D, Stroobants S, Maes A, Mortelmans L. Positron emission tomography in giant cell arteritis and polymyalgia rheumatica: evidence for inflammation of the aortic arch. Am J Med 2000;108:246–9.
22. Webb M, Chambers A, AL-Nahhas A, Mason JC, Maudlin L, Rahman L, et al. The role of ^{18}F-FDG PET in characterising disease activity in Takayasu arteritis. Eur J Nucl Med Mol Imaging 2004;31:627–34.
23. Meller J, Strutz F, Siefker U, Scheel A, Sahlmann CO, Lehmann K, et al. Early diagnosis and follow-up of aortitis with [^{18}F]FDG PET and MRI. Eur J Nucl Med Mol Imaging 2003;30:730–6.
24. Rudd JH, Warburton EA, Fryer TD, Jones HA, Clark JC, Antoun N, et al. Imaging atherosclerotic plaque inflammation with [^{18}F]-fluorodeoxyglucose positron emission tomography. Circulation 2002;105:2708–11.
25. Yun M, Yeh D, Araujo LI, Jang S, Newberg A, Alavi A. F-18 FDG uptake in the large arteries: a new observation. Clin Nucl Med 2001;26:314–9.
26. Yun M, Jang S, Cucchiara A, Newberg AB, Alavi A. ^{18}F FDG uptake in the large arteries: a correlation study with the atherogenic risk factors. Semin Nucl Med 2002;32:70–6.
27. Kerr GS. Takayasu's arteritis. Rheum Dis Clin North Am 1995; 21:1041–58.
28. Evans JM, O'Fallon WM, Hunder GG. Increased incidence of aortic aneurysm and dissection in giant cell (temporal) arteritis. A population-based study. Ann Intern Med 1995;122:502–7.
29. Liu G, Shupak R, Chiu BK. Aortic dissection in giant-cell arteritis. Semin Arthritis Rheum 1995;25:160–71.
30. Greene GM, Lain D, Sherwin RM, Wilson JE, McManus BM. Giant cell arteritis of the legs. Clinical isolation of severe diseasewith gangrene and amputations. Am J Med 1986;81:727–33.

31. Nordborg E, Bengtsson BA. Death rates and causes of death in 284 consecutive patients with giant cell arteritis confirmed by biopsy. BMJ 1989;299:549–50.
32. Meller J, Grabbe E, Becker W, Vosshenrich R. Value of F-18 FDG hybrid camera PET and MRI in early takayasu aortitis. Eur Radiol 2003;13:400–5.
33. Belhocine T, Blockmans D, Hustinx R, Vandevivere J, Mortelmans L. Imaging of large vessel vasculitis with ^{18}FDG PET: illusion or reality? A critical review of the literature data. Eur J Nucl Med Mol Imaging 2003;30:1305–13.
34. Brodmann M, Lipp RW, Passath A, Seinost G, Pabst E, Pilger E. The role of 2-^{18}F-fluoro-2-deoxy-D-glucose positron emission tomography in the diagnosis of giant cell arteritis of the temporal arteries. Rheumatology (Oxford) 2004;43:241–2.